International Research Journal of Innovations in Engineering and Technology (IRJIET)

ISSN (online): 2581-3048

Volume 9, Issue 11, pp 199-209, November-2025

https://doi.org/10.47001/IRJIET/2025.911024

The Effect of Surface Ripples on Mixed Convection between Two Cylinders with Rotating Outer Cylinder

[1]Mohammed Abdullah Bakir, [2]Ataalah Hussain Jassim

[1,2]Mechanical Engineering Department, College of Engineering, University of Mosul, Mosul, Iraq

Authors E-mail: [1]mohammed.23enp81@student.uomosul.edu.iq, [2]Ataalah.jasim@uomosul.edu.iq

***Abstract* - Numerical investigation is presented for mixed convection problem in a concentric inner sinusoidal (soft, semi- circular and square) cylinder and an outer rotating circular cylinder, which were kept at constant hot and cold temperature respectively. The governing equations are formulated and modeling in ANSYS-Fluent.21R1, a partial differential equation solver based on (FVM). The governing parameter considered are Reynolds number (50,75,100,119.5,150 and 350) for each Rayleigh number (50000,100000 and 150000) and the inner cylinder corrugation varied as (N0, SWA10, SW, SC and SQ) this study investigate the effect of varying cylindrical surface geometric – from smooth to sinusoidal soft, semi – circular, and square wave – on thermal performance as wave amplitude increases. The results revealed that gentle undulation with low Rayleigh number enhanced heat transfer by 12.6%, as a result of shear retardation and forced convection at (Re=150). When the wave amplitude was increased to 22.96 mm, the enhancement reached 32% at (Re=350). Specifically, the transition from deep undulation soft to semicircular ripple contributed to remarkable enhancements of 138% at high Rayleigh number under (Re=150). In addition, the study demonstrated that the square ripple consistently provided the most effective thermal insulation under all examined conditions.**

Keywords: Mixed convection, Concentric annular cylinders, Square ripple, Rotating cylinder, Types of ripples.

I. INTRODUCTION

The study of heat transfers by natural and mixed convection within annular spaces has been of continuing interest for decade. Convective heat transfer is clearly a field that studies the relationship between the field of heat transfer and the field of fluid mechanics the relationship between the two fields has been developed over the past century [1]. The process of heat transfers within narrow annular spaces had problems and obstacles, which negatively affected energy savings and costs [2]. To improve thermal systems that are used in many engineering applications such as refrigeration systems, thermal storage units, solar collectors, and seat bearing lubrication etc. [3,4]. These efforts included the physical and chemical properties of working fluids, using more efficient fluids, modifying the geometric shapes of the areas where heat exchange occurs [5], or the effect of surfaces with undulation in contact with the medium [3], or the rotational motion of the cylinder [6] on the fluid dynamics and heat transfer.

Sheikh al-Islam *et al.* [7] studied natural convection between a hot, wavy inner cylinder and a cold, concentric outer cylinder, the results showed that the flow pattern and heat distribution, were significantly affected by wave number, amplitude and Raleigh number, with the highest and lowest average Nusselt number values appearing at waviness 4 and 5, respectively. Qusay *et al.* [8] conducted a numerical study of fluid flow in a rippled circular enclosure, which showed that the circular shape ofthe inner cylinder is the best among the square and triangular shapes, with an improvement of 23.3% at a distance of 0.3 and a specific Raleigh number. Asad *et al.* [9] conduced a numerical study natural convection in a rippled circular, enclosure containing a heat rectangular split baffles, the results revealed a direct proportionality between the distance of baffles and average Nusselt in the horizontal and inclined position, and inverse proportion in the vertical position, with the highest value of average Nusselt at the vertical position at the bottom of the container and the lowest distance 0.215. M.S. Sadeghia *et al.* [5] performed a study on a wavy circular cavity filled with Nano fluid, and it was found that the Nusselt number increase with the Raleigh number and the radiation coefficient, and decreases with Hartmann and the distance between the two cylinder. The effect of magnetic field and thermal radiation was prominent at different Raleigh numbers.

Farooq Hassan *et al.* [10] studied the inner cylinder undulation, and it was observed that heat transfer decreases with increasing Reynolds number and undulation number, and increases with Raleigh number and concentration of Cu-H_2O nanoparticle, and that rotation enhances conduction and inhibits convection. Sree Prdip *et al.* [11] performed a numerical study of a rectangular container containing two hot bodies in three positions and it was concluded that the walls generate additional vortices and thermal plumber due to buoyancy, and that the ripples on the top wall impede conduction and produces a boundary layer and recirculation

International Research Journal of Innovations in Engineering and Technology (IRJIET)
ISSN (online): 2581-3048
Volume 9, Issue 11, pp 199-209, November-2025
https://doi.org/10.47001/IRJIET/2025.911024

zones. Abeer and Habibis [12] presented a computational analysis of a hybrid nanofluid in a rotating corrugated container, it was found that the intensity of the vortices and thermal performance improved with increasing the rotation speed, number of undulation, and concentration of NEPCMs, the performance enhance by 38% when the concentration increased from 1% to 5%. Fatin *et al.* [13] presented a numerical study which showed that the concentration of nanofluid enhances heat transfer without the need for a magnetic field, and the best performance was when natural convection dominates and the ripple number is 2, while a high Hartmann weakens heat transfer.

Despite numerous studies on sinusoidal sine ripple with soft surfaces, there remains a research gap regarding the effect of ripple shape, such as square and semi-circular. Square ripple exhibit high fluid resistance due to their sharper surface ripples compared to soft sine ripple, this difference is reflected in the mixed convection behavior.

II. THEORETICAL DETAILS

2.1 Problem Description

Figure (1) shows the physical engineering model, the inner cylinder is hot at constant temperature (T_h) and the outer one is cold (T_c) and rotates at a constant angular velocity (ω) and (g) represent gravity. Five shapes were chosen for inner cylinder, including smooth soft, square, and semi-circular ripples with amplitude of (10 and 22.96 mm) and wave number of 4, with aspect ratio 2 and (D_{inner}=120 and D_{outer}=240 mm). The function to form soft sinusoidal ripples and square sinusoidal ripples respectively.

$$X = \left[R + Asin\left(N * \phi * \frac{\pi}{180}\right)\right](\cos\left(\phi * \frac{\pi}{180}\right)) \quad (1)$$

$$Y = \left[R + Asin\left(N * \phi * \frac{\pi}{180}\right)\right](\sin\left(\phi * \frac{\pi}{180}\right)) \quad (2)\ [10]$$

$$X = [R + A * sgn(\sin(N\phi))](\cos\left(\phi * \frac{\pi}{180}\right)) \quad (3)$$

$$Y = [R + A * sgn(\sin(N\phi))](\sin\left(\phi * \frac{\pi}{180}\right)) \quad (4)$$

$$sgn(\sin(N\phi) = \begin{cases} \sin(N\phi) > 0 & if\ 1 + \\ \sin(N\phi) > 0 & if\ 0 \\ \sin(N\phi) > 0 & if\ 1 - \end{cases}$$

Where (A) is amplitude, (N) is number of undulation, and (ϕ) is the polar angle. This function relies on converting the sine function to a square function using the sign function ($sign(\sin(N\phi))$, which changes the radius abruptly between (A+) and (A-). It is worth noting that the function (square($N * \phi$)) in the MATLAB environment generate a square ripple that relies on the sin function instead of the sign function.

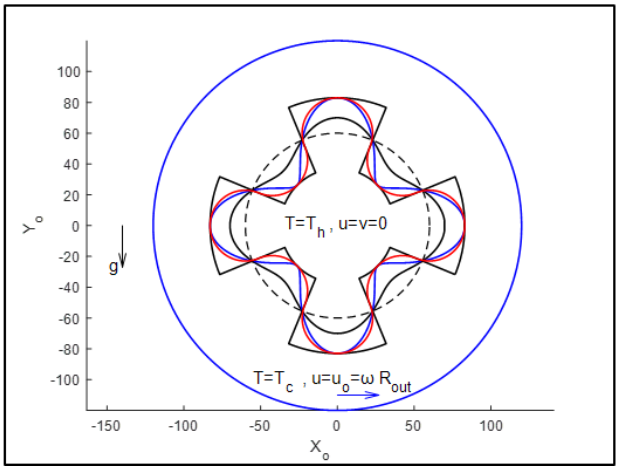

Figure (1): Shows the physical engineering model

The properties of water are:

$$(\rho = 998.2\ \ \frac{Kg}{m^3}, \mu = 0.001003\ \ \ pa.sec,\ \ K = 0.6\ \ \frac{wat}{Kg.K}, C_P = 4186\ \frac{J}{Kg.K}, \beta = 0.00021\ \ \frac{1}{K}, Pr = 6.9976)$$

2.2 Governing equation

The model assumes a two-dimensional, steady state, laminar, Newtonian flow with constant properties (ρ, μ, and K), except for density in the vertical direction (y) treated using the Boussinesq approximation, neglecting radiation and viscous dissipation, and applying no-slip condition on cylinder surfaces. In accordance with the abovementioned assumption, the governing equation dimensionless for the cavity flow between two cylinder are given as follows: continuity, X-Momentum, Y-Momentum, and Energy equation respectively.

$$\frac{\partial U}{\partial X} + \frac{\partial V}{\partial Y} = 0 \quad (5)$$

$$U\frac{\partial U}{\partial X} + V\frac{\partial U}{\partial Y} = -\frac{\partial P}{\partial X} + \frac{1}{Re}\left(\frac{\partial^2 U}{\partial X^2} + \frac{\partial^2 U}{\partial Y^2}\right) \quad (6)$$

$$U\frac{\partial V}{\partial X} + V\frac{\partial V}{\partial Y} = -\frac{\partial P}{\partial Y} + \frac{1}{Re}\left(\frac{\partial^2 V}{\partial X^2} + \frac{\partial^2 V}{\partial Y^2}\right) + Ri\,\theta \quad (7)$$

$$U\frac{\partial \theta}{\partial X} + V\frac{\partial \theta}{\partial Y} = \frac{1}{Re\ Pr}\left(\frac{\partial^2 \theta}{\partial X^2} + \frac{\partial^2 \theta}{\partial Y^2}\right) \quad (8)$$

Where the dimensional variables, and the dimensional number are:

$$X = \frac{x}{H},\ Y = \frac{y}{H},\ H = R_{out} - R_{inner},\ AR = \frac{R_{out}}{R_{inner}}$$

$$U = \frac{u}{u_0},\ V = \frac{v}{u_0},\ P = \frac{p}{\rho\ U_0^2},\ \theta = \frac{T - T_c}{T_h - T_c},\ \Psi = \frac{\psi}{u_0\ L}$$

$$\alpha = \frac{K}{\rho\ cp}, \nu = \frac{\mu}{\rho}, Pr = \frac{\nu}{\alpha}, u_0 = \omega\ R_{out}, \bar{R}_{out} = \frac{R_{out}}{H}$$

International Research Journal of Innovations in Engineering and Technology (IRJIET)

ISSN (online): 2581-3048

Volume 9, Issue 11, pp 199-209, November-2025

https://doi.org/10.47001/IRJIET/2025.911024

$$Ra = Gr * Pr, Ra = \frac{g\,\beta\,(T_h - T_c)H^3}{\alpha\,\nu},\ Re = \frac{U_0\,H}{\nu},\ Ri = \frac{Gr}{Re^2}$$

[14], [15]

In fluid mechanics, the fluid motion can be described using the stream function Ψ, which is derived from the velocity components U and V.

$$U = \frac{\partial \Psi}{\partial Y},\quad V = -\frac{\partial \Psi}{\partial X} \qquad (9)\ [10]$$

To study further the mixed conviction characteristics, outcomes for both local, Nu_{Loc} and average, Nu_{avg} around the inner heated cylinder are also significant in the heat transfer system, as following[14]:

$$Nu_{Loc} = \frac{\partial \theta}{\partial r}, Nu_{avg} = \frac{1}{2\pi}\int_0^{2\pi} Nu_{Loc}\ (\phi)\ d\phi \qquad (10)$$

The non-dimensional boundary conditions used in this study are given as follows:

At inner cylinder R = R_{inner} ,

$\theta = 1$, and $U = V = 0$ (11)

At outer cylinder $R = R_{out}$,

$\theta = 0$, and $U = U_0 = \Omega\,\bar{R}_{out} = \sqrt{U_{oy}^2 + V_{ox}^2}$ (12)

$U_{0Y} = -\Omega\,(Y - Y_o),\ V_{0X} = \Omega(X - X_o)$ (13) [14]

III. Numerical Scheme

3.1 Numerical solution

The non-dimensional governing equation (eq. 5-8) with boundary condition (eq. 11-12) were solved using the control volume approach in ANSYS-Fluent.21R1. Spalding and Patankar's SIMPLE algorithm [16] was employed for pressure-velocity coupling, with a second order upwind scheme for better accuracy. Convergence and stability were ensured by adjusting the under-relaxation factor (0.3-1), and a convergence criterion of 10^{-5} was applied to minimize numerical errors.

Mesh in D_{inner}Mesh 0.5 Mesh in D_{outer}

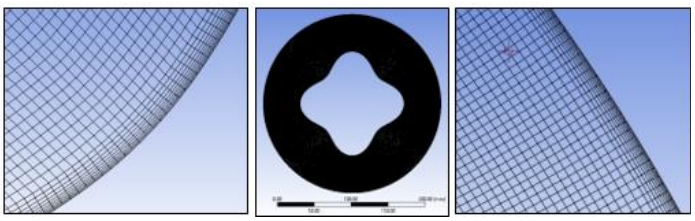

Figure (2): Shows the mesh generation with the areas near the cylinder walls enlarged

3.2 Grid Independence test

A mesh generated with finer cells and element near the lines of heated inner cylinder and the rotating cylinder of the Quadratic type to fit all shapes as in Figure (2). The study of the independence of the rubber mesh was carried out using (SWA10) at (Re=100, Ra=10^5), with a number of elements from 9367 to 255386. Table (1) showed that average Nusselt stabilizes at 19865 for the typical model only, but a mesh of 163109 with an element size of 0.5 was used to the accuracy, efficiency, and stability of both the average Nusselt and stream function together, and it was adopted in all subsequent simulations.

Table (1) shows the values of (Nu_{avg}) and (Ψ_{max})

Numb.of element	Nu_{avg}	Δ (%)	Ψ_{max}	Δ (%)
9367	5.731	-	205.987	-
19865	4.443	22.466	161.214	21.736
45529	4.461	0.393	147.138	8.731
163109	4.470	0.199	137.632	6.461
206589	4.462	0.166	136.717	0.665
255386	4.445	0.387	137.916	0.877

3.3 Validation

To validate the code in ANSYS-Fluent.21R1, the results of average Nusselt number and stream function were compared with previous studies (Khanafer [17] and Roslan [18]), the comparison showed good agreement at several values of Raleigh, prantl 6.2 for water and (R=0) as shown in table (2). Also, the second case of Nusselt number and the heat distribution were compared with Roslan's study at (R=0.2, Pr=6.2, 100=Ω, Ra=10^5), the result showed good agreement.

Table (2)

Ra	Present study Nu_{avg}	Khanafer [17] Nu_{avg}	Roslan et al. [18] Nu_{avg}
10^3	1.066	1.12	-
10^4	2.135	2.299	2.272
10^5	4.834	4.72	4.716
10^6	9.784	9.688	-

International Research Journal of Innovations in Engineering and Technology (IRJIET)

ISSN (online): 2581-3048

Volume 9, Issue 11, pp 199-209, November-2025

https://doi.org/10.47001/IRJIET/2025.911024

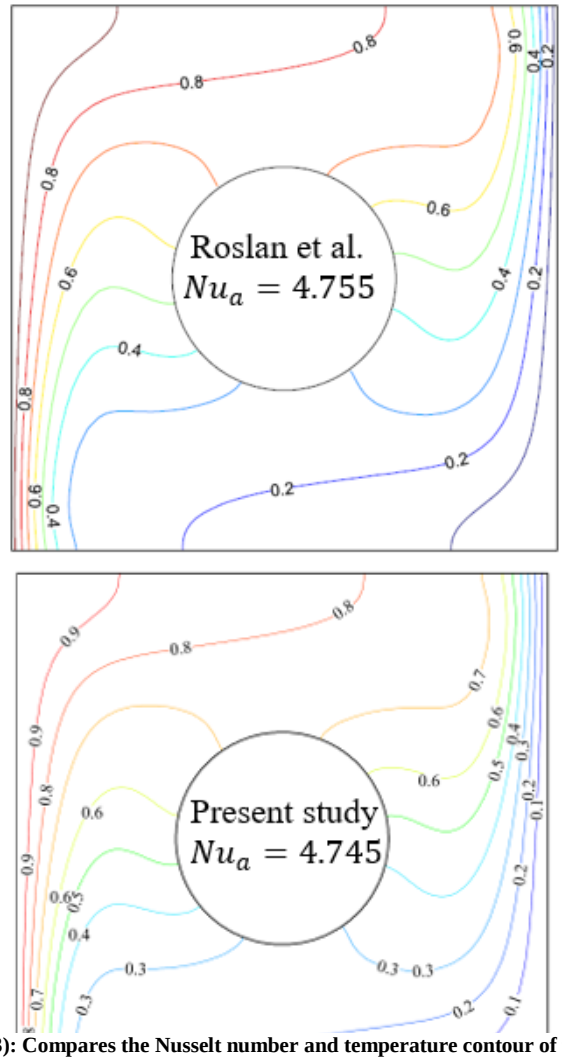

Figure (3): Compares the Nusselt number and temperature contour of the present study with Roslan et al.

IV. RESULT AND DISCUSSION

The wavenumber was fixed at (N=4) with the inner cylinder shape varied from smooth to soft, semicircular, and square ripple with different amplitude to assess the effect of waviness and surface roughness on heat transfer.

4.1 Influence of Rayleigh number and Geometry on the stream function and isotherms contours

All cases were simulated at Re=119.5 with three Rayleigh number (50000,100000 and 150000) and the corresponding value of Richardson number (0.5, 1 and 1.5). Figure (4) illustrate the effect of the corrugated surface shape on the flow patterns and heat distribution inside the circular gap.

In general, increasing the Rayleigh numbers reduces stream function and thermal plumber thickness, enhancing heat transfer. A single vortex forms with moderate performance (Nu_a=2.5) at low Rayleigh and (Ri=0.5), this cell was generated due to upward thermal buoyancy, then descended along the outer cylinder as the cooled fluid particles become denser, the inner cylinder's rotation enhanced the vortex on the left side but weakened on the right. Multiple vortex appear that enhance natural convection at moderate Rayleigh and (Ri=1). At high Rayleigh and (Ri=1.5) natural convection becomes dominant, raising the Nusselt to 5 and achieving the best thermal performance despite the smooth surface (N0) due to strong buoyancy effect.

In wavy geometry (SWA10), undulation caused cell division and stimulated interaction between the two convective forces, slightly improving heat transfer at low Rayleigh number. As the Rayleigh increases, multiple cells appeared and the Nusselt increased to 4.99. But at high Rayleigh, the effect of undulation was limited with natural convection dominating the thermal performance. In wavy pattern (SW), increasing amplitude led to the appearance of complex, overlapping vortex cells, reducing convective efficiency despite partially improving the stream function. As the Rayleigh increased, the Nusselt improved due to bouncy force, but its reducing compared to lower amplitude due to cell crowding and heat trapping in the grooves.

In the semicircular form (SC), the undulation increasing flow turbulence without improving heat transfer at low Rayleigh. As Rayleigh increased natural convection was activated and the Nusselt number gradually increased, but performance remained lower than (SWA10) due to roughness and high amplitude which promote heat retention. In the square ripple (SQ), sharp corners and internal undulation led to flow dispersion and heat retention, reducing the average Nusselt number to lowest value of 1.48 at low Rayleigh. As Rayleigh increased, heat transfer improved somewhat but remained poor compared to soft undulation due to thermal insulation and surface roughness that trapped convection currents within the grooves. This shape recorded the lowest thermal efficiency among all configuration.

Overall, across all shapes, the Nusselt number improved by 30-35% when the Rayleigh number increased from low 50000 to moderate 100000, and By 16-21% from moderate 100000 to high 150000.

4.2 Influence of Reynolds number and Geometry on the stream function and isotherm contour

Physical analysis and comparison of the effect of external cylinder rotation with Reynolds (50,150,350) and internal shape change (N0, SWA10, SW, SC, SQ) on flow and heat transfer, at low, and high Rayleigh number through the contour stream function with its maximum value and minimum dimensionless (Ψ_x, and Ψ_i), and the contour temperature distribution & average Nusselt as illustrated in figures (5), and (6).

ISSN (online): 2581-3048
Volume 9, Issue 11, pp 199-209, November-2025
https://doi.org/10.47001/IRJIET/2025.911024

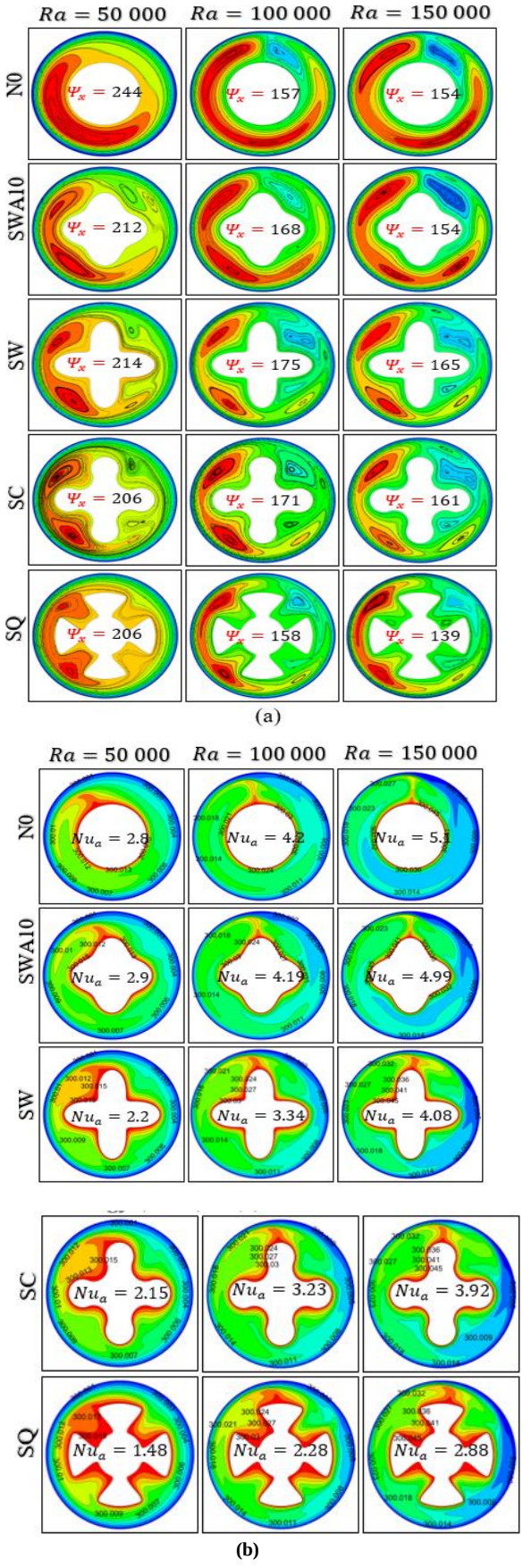

Figure (4): Illustrates (a) contour stream function (b) contour temperature distribution under the influence of levels Rayleigh number with variation shapes for (Re=119.5)

In the reference shape (N0), at (Re=50) a strong natural convection pattern appeared with more than one vortex cell and a high Nusselt of 4.2, and 5.4, for low, and high Rayleigh respectability. As Reynolds increased to 150, forced convection began to dominate and the decreased to 2.2, and 4.5 at low & high Rayleigh. At Reynolds 350, the cells completely disappeared at low Rayleigh, the flow become hoop-like, the Nusselt decreased sharply to 1.4, and 1.8 for Rayleigh (low, and high) due to the dominance of hydrodynamic shear. Accordingly, the heat transfer rate (Nu) exhibited a reduction of 65.4%, and 66% at the two Rayleigh number levels within the range of 50-350.

In geometry (SWA10), the soft undulation maintained the normal cells at Reynolds 50 with a winder thermal plumber and Nusselt of 3.9, and 5.1 with increasing Rayleigh levels. As Reynolds increased to 150, additional cells appeared and stream function increased, but the Nusselt decreased slightly, while a 12.6% improvement compared to the smooth surface at low Rayleigh. At Reynolds 350, the Nusselt decreased to 1.5, and 2.3 due to high speed, with further improvement with increasing Rayleigh levels of 4.6%, and 27% compared to the smooth surface. The overall improvement due to different the smooth and undulation collapses were 4%, and 11%for speed between 50 and 350.

In form (SW), increased amplitude led to heat retention in the groove, reduced the Nusselt to 3.1, and 4.2 at Reynolds 50. As Reynolds rose to 150, flow become confined and causing Nusselt drops of 41.9%, and 66% due to the dominance of early forced convection. At Reynolds digit 350, the bursting of the confined cells caused local turbulence with a massive jump in the stream function to 9246, and 8806 with increased Rayleigh, raising the Nusselt to 2, and 1.82, the efficiency improves by 32% under low Rayleigh due to raising amplitude, and by 38% compared to the smooth surface.

In the semicircular (SC) with difference roughness, increasing the Reynolds between (50-150) resulted in varied in number of cells with raising the stream function and dropping the Nusselt to 1.89, and 3.5 with increasing Rayleigh, but with an improvement of Nusselt by 26.6%, and 138% compared to (SW) at Re=150 for low, and high Rayleigh because it resisted early forced convection. The overall improvement in thermal collapse resistance at speed (50-150) is 53% at high Rayleigh due to semicircular type compared to (SW) at Re=350 four vortex cells appear with circular thermal gradient distribution reflected a weak and confined convection.

ISSN (online): 2581-3048
Volume 9, Issue 11, pp 199-209, November-2025
https://doi.org/10.47001/IRJIET/2025.911024

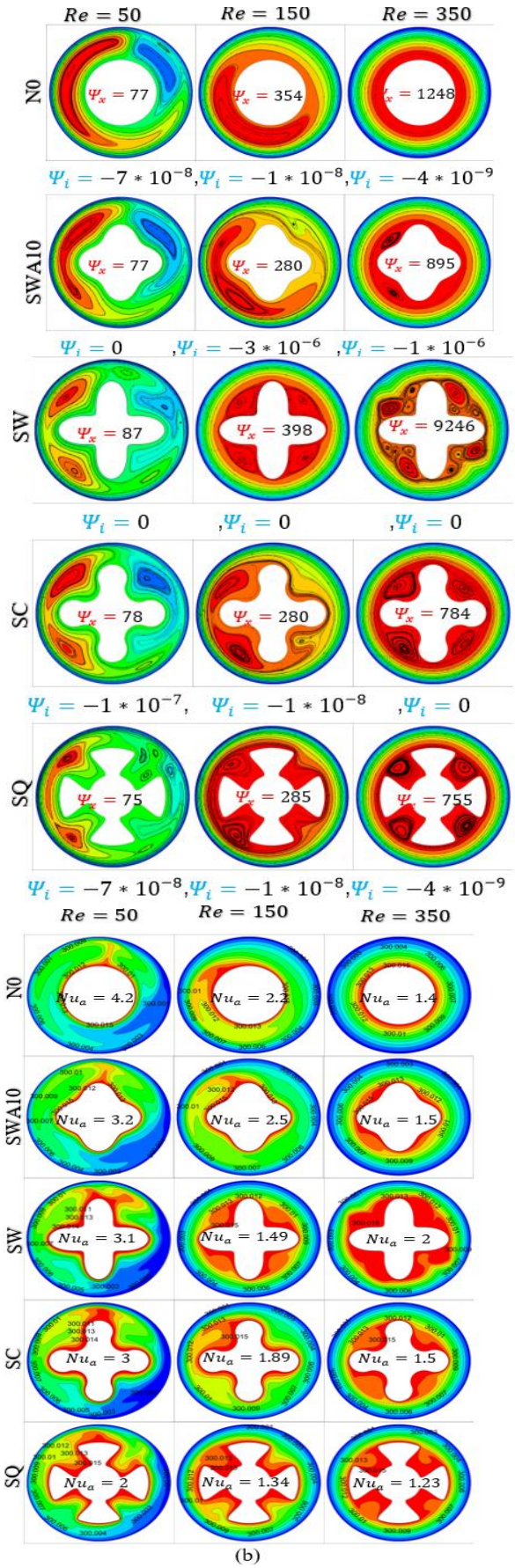

Figure (5): (a) contour stream function (b) contour temperature distribution, under the influence of four Reynolds (50, 150, 350) for Rayleigh (50000) for all shapes

In geometry (SQ), the square ripple caused that pockets trapping led to a decrease in the Nusselt to 2.09, and 3.03 at Re=50, despite the increased boundary layer thickness within pockets. As Reynolds 350. The Nusselt continued to weaken to 1.23, and 1.3, making this shape the lowest thermal performance in all cases and suitable for insulation.

4.3 Local and average Nusselt number

Figure (7) illustrates the effect of Reynolds and Rayleigh number on the local Nusselt number distribution along the circumference of the hot inner cylinder for each shape. The local Nusselt is plotted as a function of the circumferential angle (ϕ) from 0 to 360 in the clockwise direction.

In the smooth configuration (N0) the local Nusselt increases up to an angle (80^o) due to heat accumulation and weak convection, then decreases up to (280^o) due to arising thermal plumber and an increasing boundary layer, before rising again to 360^o at Reynolds 150 the peak shift to 0^o as it decreases, while at Re=350 the vales (peaks and troughs) converge due to the dominance of forced convection.

In the ripple soft (SWA10), the local Nusselt is highest between 350^o-150^o due to heat retention and weak convection where a peak occurs at an angle of 60^o, in contrast, a decrease is observed between 150^o -350^o due to the appearance of the thermal plumber and the increases thickness of the boundary layer thickness, in addition to the role of the vortex cells that enhanced the local heat transfer, which led to the values Nu_{loc} dropping to the minimum at the angle 250^o.The paradox caused by the subtle ripple at Reynolds 350 is that the peaks and troughs do not converge due to the grooves and vortex cells, which separate the thermal boundary layer from the hot wall and increase its thickness, especially at high Rayleigh.

In the soft ripples (SW) with (A=22.96), it is clear that the Nu_{loc} increase significantly in the angular range 350^o-150^o the direct flow impinges on the surface at 330^o, creating a thin boundary layer and a steep thermal gradient, raising the Nusselt. The values gradually decrease until the stagnation zone due to the flow divergence at 350^o, the decrease continues until an angle of 20^o, at 60-70^o, a local peak appears resulting from the separation of two vortex cells and the pressure of the flow towards the surface, which raises the thermal gradient and reduces the thickness of the boundary layer. The troughs in the local Nusselt curve indicate areas of strong interaction between the flow and the hot surface, which leads to enhanced heat transfer in those area, while the peaks indicate thermal accumulation resulting from the weak ability of the flow to remove heat, and somewhere even press the fluid towards the hot surface, this is usually associated with a decease in the thickness of thermal boundary layer and the

International Research Journal of Innovations in Engineering and Technology (IRJIET)

ISSN (online): 2581-3048

Volume 9, Issue 11, pp 199-209, November-2025

https://doi.org/10.47001/IRJIET/2025.911024

formation of a sharp gradient that limits the efficiency of convection.

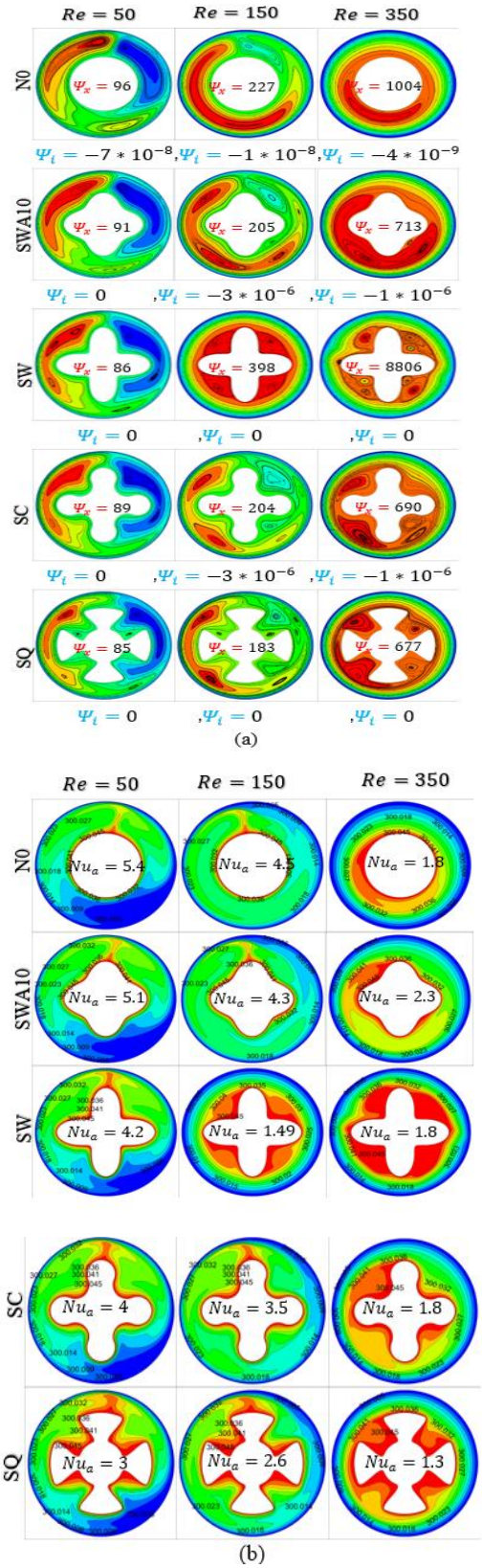

Figure (6): (a) contour stream function (b) contour temperature distribution, under the influence ofReynolds (50, 150, 350) for Rayleigh (150000) for all shapes

In semi-circular ripple (SC) with (A=22.96), at angle of 210^o a thin boundary layer are observed due to the direct collision of fluid with the hot wall, but the Nusselt is not yet at its peak. At an angle of 240^o, the fluid moves over the convex surface towards the concave one, expanding the gap and forming cells, increasing the heat mixing and transfer, and reducing Nu_{loc}. When the angle reaches 290^o, the boundary layer is compressed by the flow more to record the highest Nu_{loc}. Thus the process is repeated between rising and falling at the convex and concave ones, respectability.

In the (SQ) with (A=22.96), square ripple led to very strong heat retention and accumulated gradient and thin boundary layer at low speed between the angle (0-180^o), especially at 60^o, recording the highest local Nusselt value of 15.3 even among the other shapes. It also records the lowest Nusselt value of the curves, with strong troughs for each groove, as result of the separation of the boundary layer from the hot body, a wide thermal plumber with spread thermal gradient, thanks to the nature of the geometric shape especially in the upper part of the cylinder. At the high speed in forced convection, the peaks and troughs are alternating and regular.

In general, for all cases, the higher the Rayleigh value, the higher the local Nusselt value, regardless of the difference between the peaks and troughs of each shape. The higher Reynolds, the smaller the difference between the peaks and the troughs in the curves. It also takes on wavy geometric shape, especially the soft one.

Figure (8) (a) (b) (c), when the rotational speed of outer cylinder increases with Reynolds from 50 to 350, the average Nusselt number decreases sharply at low Rayleigh due to the weakness the natural convection as a result of the shear resulting from the forced flow, while at moderate Rayleigh, resistance to this decrease is shown, and a balance between the natural convection and forced flow (mixed convection) appears during speed (50-119.5).

At a high Rayleigh, it rises and grows slightly, then decreases by a small value because the thermal buoyancy force is strong enough to resist the effect of shear at speed (50-119.5) for all shape, except for shape (SW), which has deep soft ripple when the Reynolds reaches 150 its value decreases and it collapse and the severity of its collapse increases with the increase in Rayleigh number due to the dominance of early forced convection. When the speed continues from 150 to 350, all shapes under the influence of all Rayleigh values to decrease, except for shape (SW) where the average Nusselt increases, it outperforms other shapes in thermal performance, especially at low Rayleigh because the forces flow began to completely dominate and worked to activate the flow and the

International Research Journal of Innovations in Engineering and Technology (IRJIET)
ISSN (online): 2581-3048
Volume 9, Issue 11, pp 199-209, November-2025
https://doi.org/10.47001/IRJIET/2025.911024

collision of the four cells in the groove with the walls of the deep ripple to form many cells confined in the groove with a circular flow collar with a huge and strong jump in the stream function to reach about 9000, which contributed to the clear separation of the thermal boundary layer from the hot wall.

Referring to figure (4-6) (d) for the soft ripple, with increase in amplitude from 10 to 22.96 mm, it is noted that the Nusselt decrease across all Rayleigh values. A sudden collapse of the Nusselt to 1.5, under a speed 150, occurs simultaneously across the various Rayleigh values. While it improves at Reynolds 350, due to the sharp change in the dominance of forced convection and the decline in natural convection to the point of cancellation, with the creation of several vortex cells that help separate the boundary layer, leading to a transformation of the heat transfer to a pattern closer to traditional strong thermal conduction.

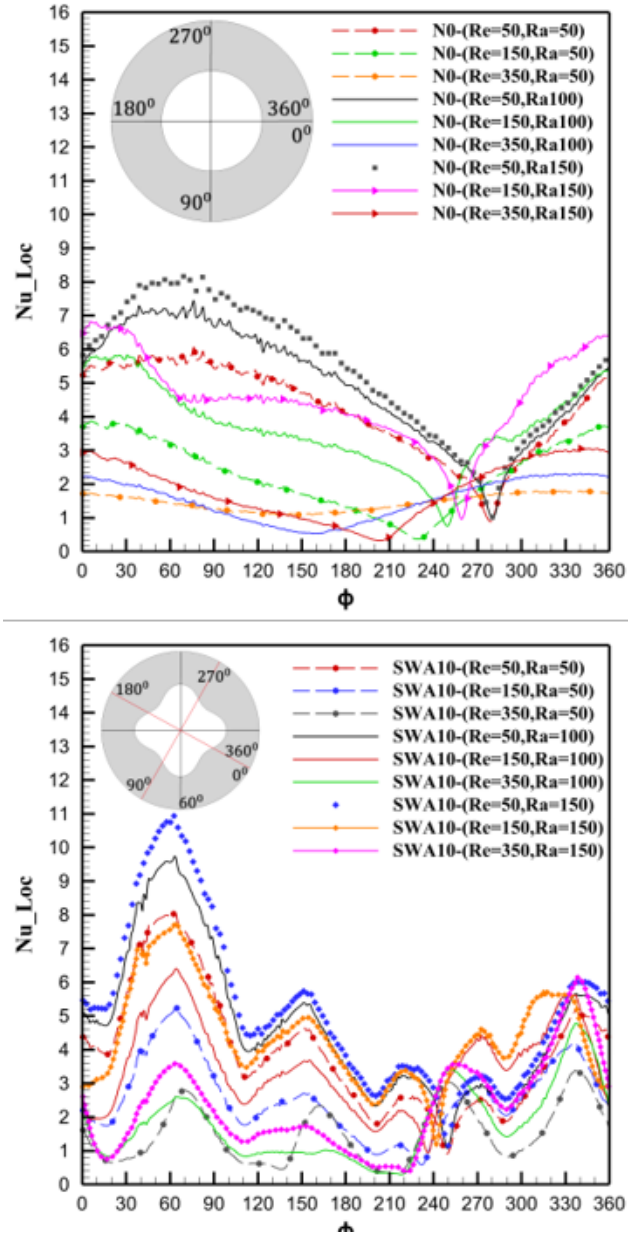

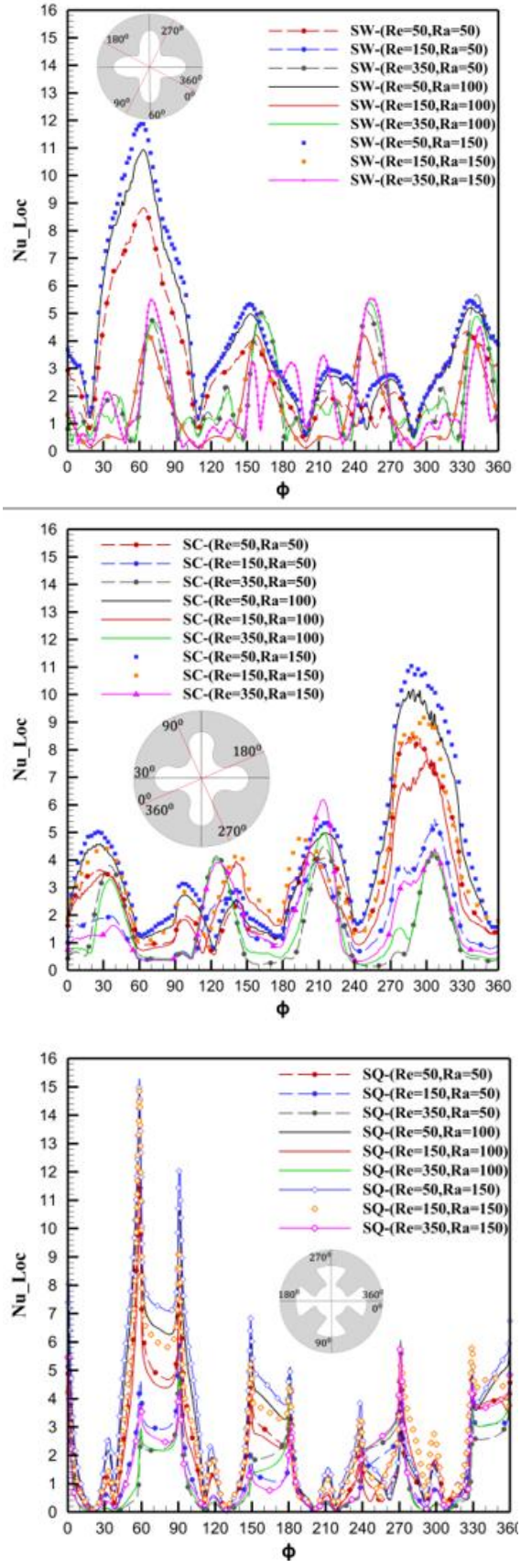

Figure (7): Illustrate the local Nusselt number for three values of Reynolds (50, 150, 350) for each Rayleigh (Ra*10^3) for all shapes

International Research Journal of Innovations in Engineering and Technology (IRJIET)

ISSN (online): 2581-3048

Volume 9, Issue 11, pp 199-209, November-2025

https://doi.org/10.47001/IRJIET/2025.911024

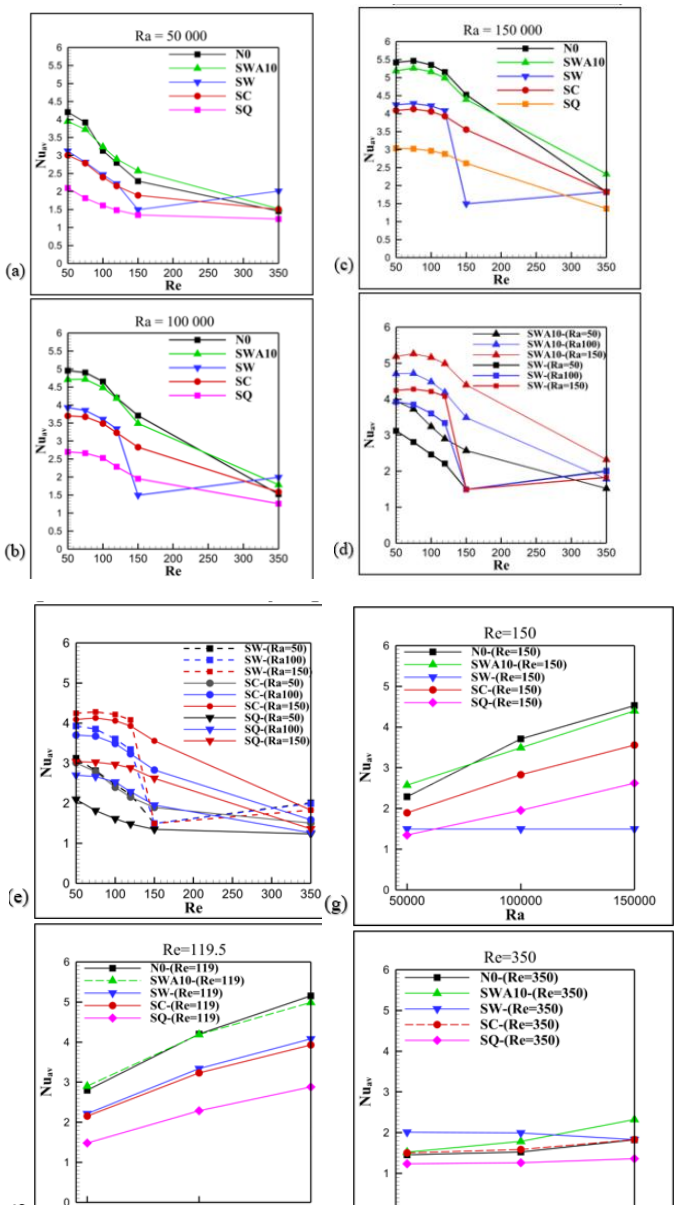

Figure (8): Illustrate (a-e) average Nusselt function of Reynolds, average Nusselt function of Rayleigh, for all shapes

Figure (4-6) (e) illustrate the effect of the roughness ripple with amplitude 22.96 mm such as (SW, SC, SQ), A good decrease in the thermal performance is observed in the square ripple in all condition, while the semicircular ripple have a thermal behavior similar to the square ripple but with the higher Nusselt value and closeness to the soft ripple value, and a good improvement when the speed reaches 150 compared to the soft ripple due to their sudden collapse.

Figure (8) (f) (g) (h) illustrate the effect of the average Nusselt as a function of the Rayleigh, it is evident that the higher the Raleigh value, the higher the Nusselt values for low speeds for all shapes. The sudden collapse of the deep ripple (SW) for the Nusselt at Reynolds 150 showed its stability and slight decrease when the Rayleigh levels were raised, while its value decrease further when the speed reach 350 with a jump from the worst to the best thermal performance compared to the rest of the shapes, except for the subtle ripple for the high Raleigh, which is the best. It was also noted that the Rayleigh value have a clear effect on the average Nusselt at low speeds, while it is almost negligible when the speed reaches 350 due to the tight grip of the forced convection on the system with the disappearance of natural convection, so that thermal conduction become dominant.

V. CONCLUSIONS

In this numerical analysis, the effect of inner cylinder ripples on heat transfer with outer cylinder rotation for mixed convection study was investigated, through simulation over a range of Reynolds number (50-350) and Rayleigh number (50000-150000). The inner cylinder geometry configuration included five shapes (N0, SWA10, SW, SC, SQ) and wavenumber of 4. The analysis revealed the following main results:

1. At low speeds (Re=50), natural convection dominates and the smooth shape achieves the highest Nusselt number (4.2).
2. Subtle ripple (SWA10) achieve a good balance between mixing and thermal performance, especially at low and medium speeds to give the best thermal performance.
3. Deep ripple (SWA22.96) are effective at high speeds (Re=350) thanks to local mixing enhancement.
4. Deep ripples (SCA22.96, and SQA22.96) impede flow and impair heat transfer, except for the shape (SWA22.96) at high speeds 350 where it went from worst to best.
5. Increased Rayleigh, enhanced convection, generated multiple and more complex vortex cells and thinned thermal plumber, indicating higher thermal efficiency and Nusselt.
6. Surface shape has a significant effect at low and moderate Rayleigh, while at high Rayleigh the effectiveness of the undulation is weakened and the natural convection become the main factor for heat transfer performance.
7. Sharp undulation such as (SQA22.96) impair heat transfer and create reverse flow turbulence, regardless of the intensity of the natural convection.
8. High amplitude increase flow complexity and create additional sub-cells, but it does not guarantee thermal improvement. Rather, it may lead to convection distortion and increased thermal plumber thickness with its retention, thus reducing efficiency.

Recommendations

Several suggestions could be applied in future studies, namely:

1. Apply this study practically and compare the practical results with the theory.

ISSN (online): 2581-3048
Volume 9, Issue 11, pp 199-209, November-2025
https://doi.org/10.47001/IRJIET/2025.911024

2. Research study but with the rotation of the inner cylinder and the addition of nanomaterials to the working fluid.
3. Investigation of square ripples for thermal insulator enhancement by incorporating a phase change material (paraffin), identified as the most effective insulator based on the results.

ACKNOWLEDGEMENT

The authors gratefully acknowledge the mechanical engineering department, University of Mosul, for their continuous academic support and encouragement throughout the completion of this numerical CFD study.

REFERENCES

[1] Bejan, Adrian," Convection heat transfer", *John Wiley & sons*, 2013.P.1.

[2] Usman, et al. "A forced convection of water aluminum oxide nanofluid flow and heat transfer study for a three dimensional annular with inner rotated cylinder.", *Scientific Reports* 12.1 (2022): 16735.

[3] Al-Amir, Qusay Rasheed, Farooq Hassan Ali Alinnawi, and Qusay Adnan. "Computational Study of Mixed Heat Convection in Annular Space between Concentric Rotating Inner and Wavy Surface Outer Cylinders." *Pertanika J. Sci. Technol.* 27 (2019): 1991-2013.

[4] Shih, Y-C., et al. "Periodic fluid flow and heat transfer in a square cavity due to an insulated or isothermal rotating cylinder.", vol. 131, Nov. (2009): 111701.

[5] Sadeghi, M. S., et al. "Analysis of thermal behavior of magnetic buoyancy-driven flow in ferrofluid–filled wavy enclosure furnished with two circular cylinders." *International Communications in Heat and Mass Transfer* 120 (2021): 104951.

[6] Yoo, Joo-Sik. "Mixed convection of air between two horizontal concentric cylinders with a cooled rotating outer cylinder." *International journal of heat and mass transfer* 41.2 (1998): 293-302.

[7] Sheikholeslami, M., et al. "Numerical study of natural convection between a circular enclosure and a sinusoidal cylinder using control volume based finite element method." *International journal of thermal sciences* 72 (2013): 147-158.

[8] Mahdi, Qusai A., Mohammed K. Hamza, and Nawar SA Bakly, "Study of the Impacts of Different Geometry and Aspect Ratio Hot Body on Natural Convection Heat Transfer.", *International Review of Aerospace Engineering*, Vol. 15, N. 5 (2022).

[9] Ali, Asad, et al. "Investigating the thermodynamic optimization of naturally convective flow in a corrugated enclosure: The influence of gap spacing and orientation of split baffles." *Heliyon*, volume 10, August 15 (2024).

[10] Ali, Farooq Hassan, Hameed K. Hamzah, and Ammar Abdulkadhim. "Numerical study of mixed convection nanofluid in an annulus enclosure between outer rotating cylinder and inner corrugation cylinder." *Heat Transfer—Asian Research* 48.1 (2019): 343-360.

[11] Sarker, Sree Pradip Kumer, Mohammad Mahmud Alam, and Mohammod Jahirul Haque Munshi. "Simulating Mixed Convection in a Lid-Driven Wavy Enclosure with Block in Different Locations."

[12] Alhashash, Abeer, and Habibis Saleh. "Impact of Convection and Rotation on Advanced Thermal Energy Storage Using Nanoencapsulated Phase Change Materials in Wavy Enclosures." *International Journal of Energy Research* 2024.1 (2024): 7408024.

[13] Azizul, Fatin M., et al. "MHD mixed convection and heatlines approach of nanofluids in rectangular wavy enclosures with multiple solid fins." *Scientific Reports* 13.1 (2023): 9660.

[14] Hamzah, Hudhaifa, et al. "Hydrothermal index and entropy generation of a heated cylinder placed between two oppositely rotating cylinders in a vented cavity." *International Journal of Mechanical Sciences* 201 (2021): 106465.

[15] Das, Prosenjit, and Mohammad Arif Hasan Mamun. "Predicting MHD mixed convection in a semicircular cavity with hybrid nanofluids using AI." *Heliyon* 10.19 (2024).

[16] Pearson Education Limited "An introduction to computational fluid dynamics" H K Versteeg and W Malalasekera, p.186, *2nd edition 2007, Harlow, Essex CM20 2JE, England*.

[17] Khanafer, Khalil, Kambiz Vafai, and Marilyn Lightstone. "Buoyancy-driven heat transfer enhancement in a two-dimensional enclosure utilizing nanofluids." *International journal of heat and mass transfer* 46.19 (2003): 3639-3653.

[18] Roslan, R., H. Saleh, and I. Hashim. "Effect of rotating cylinder on heat transfer in a square enclosure filled with nanofluids." *International Journal of Heat and Mass Transfer* 55.23-24 (2012): 7247-7256.

NOMENCLATURE

C_P Specific heat at constant pressure (KJ/kg·K)
g gravitational acceleration (m/s^2)
K thermal conductivity (W/m·K)
N number of corrugations
Nu_a average Nusselt number of the hot inner cylinder
Nu_Loc local Nusselt number around hot inner cylinder
P dimensionless pressure
p pressure (Pa)

ISSN (online): 2581-3048
Volume 9, Issue 11, pp 199-209, November-2025
https://doi.org/10.47001/IRJIET/2025.911024

Pr Prandtl number (νf/αf)
Ra Rayleigh number (gβf L ΔT/νf αf)
Re Reynolds number
R_{inner} circle radius inner cylinder (m)
R_{out} circle radius outer cylinder (m)
T temperature (K)
Tc temperature of the cold surface (K)
Th temperature of the hot surface (K)
U dimensionless velocity component in x-direction
u velocity component in x-direction (m/s)
V dimensionless velocity component in y-direction
v velocity component in y-direction (m/s)
X dimensionless coordinate in horizontal direction
x Cartesian coordinates in horizontal direction (m)
Y dimensionless coordinate in vertical direction
y Cartesian coordinate in vertical direction (m)
N0 smooth inner cylinder without ripple
SWA10 sinusoidal wave soft with amplitude 10 mm
SW sinusoidal wave soft with amplitude 22.96 mm
SC sinusoidal wave semicircular with amplitude 22.96 mm
SQ sinusoidal wave square with amplitude 22.96 mm

GREEK SYMBOLS

α thermal diffusivity (m^2/s)
θ dimensionless temperature (T-Tc/ΔT)
ψ dimensional stream function (m^2/s)
Ψdimensionless stream function
Ψ_x Maximum dimensionless stream function
Ψ_i Minimum dimensionless stream function
μ dynamic viscosity (kg.s/m)
ϕ angle of circular cylinder (deg)
A amplitude
ν kinematic viscosity (μ/ρ) (Pa. s)
ΔT temperature difference
β volumetric coefficient of thermal expansion (K^{-1})
ρ density (kg/m^3)
ω angular velocity

ORCID
My Name https://orcid.org/0009-0009-0723-5607

Citation of this Article:

Mohammed Abdullah Bakir, & Ataalah Hussain Jassim. (2025). The Effect of Surface Ripples on Mixed Convection between Two Cylinders with Rotating Outer Cylinder. *International Research Journal of Innovations in Engineering and Technology - IRJIET*, 9(11), 199-209. Article DOI https://doi.org/10.47001/IRJIET/2025.911024

****

